Visualization of Cosmological Point-Based Datasets

Paul Arthur Navrátil*
Texas Advanced Computing Center
University of Texas at Austin

Jarrett L. Johnson†
Department of Astronomy
University of Texas at Austin

Volker Bromm‡
Department of Astronomy
University of Texas at Austin

ABSTRACT

We describe our visualization process for a particle-based simulation of the formation of the first stars and their impact on cosmic history. The dataset consists of several hundred time-steps of point simulation data, each approximately 500MB in size. For each time-step, we interpolate the point data onto a regular grid using a method taken from the radiance estimate of photon mapping[7]. We import the resulting regular grid representation into ParaView[10], with which we extract isosurfaces across multiple variables. Our images provide insights into the evolution of the early universe, tracing the cosmic transition from an initially homogeneous state to one of increasing complexity. Specifically, our visualizations capture the build-up of regions of ionized gas around the first stars, their evolution, and their complex interactions with the surrounding matter. These phenomena were not clearly visible with other visualization techniques. These observations will guide the upcoming *James Webb Space Telescope*, the key astronomy mission of the next decade.

Keywords: Interpolation, Isosurface, Astronomy, Cosmology.

Index Terms: I.3.6 [Computing Methodologies]: Computer Graphics—Methodology and Techniques; J.2 [Computer Applications]: Physical Sciences and Engineering—Astronomy

1 INTRODUCTION

One of the most important open questions in modern cosmology is to understand how the first stars in the universe, formed a few 100 million years (100 Myr) after the Big Bang, ended the so-called "cosmic dark ages"[1]. The first stars transformed the early universe from its simple, homogeneous initial state to one of increasing complexity, thus setting the stage for the entire subsequent history of structure and galaxy formation. This crucial transformation is concerned with two interrelated processes: the re-ionization of the universe, and the enrichment with heavy chemical elements. The universe before the formation of the first stars consisted of neutral, almost pure hydrogen and helium gas. Prior to the first stars, there were no sources of ultraviolet (UV) photons yet, which are required to ionize hydrogen, and the cosmic gas was completely neutral at this early time. Observations, however, have shown that the universe was again highly ionized, at least beginning one billion years after the Big Bang. How this so-called re-ionization happened is a primary focus of current cosmological debate. The universe underwent a second formative transformation at the end of the dark ages, when the pristine cosmic gas, containing only the hydrogen and helium produced in the Big Bang, was enriched with heavy chemical elements that were synthesized in the first stars, and subsequently dispersed in extremely energetic supernova explosions. The first stars, therefore, began the long nucleosynthetic process that resulted in all the heavy elements that we find in our Solar System today.

Both of these cosmic transformations were highly complex, involving the three-dimensional evolution of dark matter and gas, coupled together by gravity. Furthermore, studying the impact of the first stars on their surroundings requires a radiation-hydrodynamics calculation, which is at the frontier of what is currently feasible. Progress can therefore only be made with sophisticated, large-scale numerical simulations. Specifically, we use a Lagrangian, particle-based technique to evolve the cosmic gas, the so-called smoothed particle hydrodynamics (SPH) algorithm. Gravitational forces, acting on both gas and dark matter, are solved with a hierarchical tree method. Our code has been parallelized with the Message-Passing Interface (MPI) library, and performs well on large Beowulf-type systems.

From this simulation, we want to produce images of smooth isosurfaces that represent the various gas structures present. The particle data from the simulation has unknown structure, which hinders direct extraction of isosurfaces. Instead, we use an interpolation similar to the three-dimensional radiance estimation technique from photon-mapping[7] to interpolate the particle data to the vertices of a regular grid. In our process, the user may define the grid resolution and sampling range, which allows data to be represented at various levels of detail. With data on a regular grid, we can use any of a variety of open-source software tools to extract and view the isosurfaces. For the images presented here we use ParaView[10], which provides a feature-rich set of tools to create and enhance our images, including isosurface extraction and smoothing.

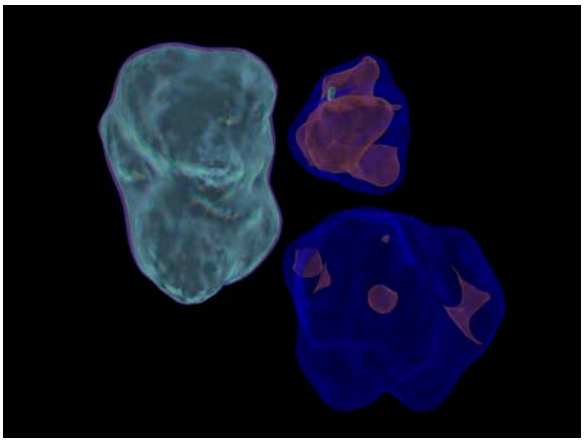

Figure 1: Regions Ionized by the First Three Stars — This figure shows the ionized gas within the first three ionized regions. A region containing an active star is on the left, while in the two regions on the right the central stars have turned off and the electron fraction is dropping as the gas recombines. Three isosurfaces of the electron fraction are shown: 0.34 (cyan), 0.10 (orange) and 0.01 (blue). The structures in the two right-most bubbles demonstrate that ionized gas cools and recombines non-uniformly, again becoming neutral. It was often previously assumed that the gas recombined in a homogeneous fashion, with the electron fraction roughly equal throughout the ionized regions.

*e-mail: pnav@tacc.utexas.edu
†e-mail:jljohnson@astro.as.utexas.edu
‡e-mail:vbromm@astro.as.utexas.edu

A key aspect of current research on the first stars is related to the build-up and growth of bubbles of either ionized gas or hot, heavy element-enriched gas. Our visualizations are crucial to elucidate the evolution of the bubbles, their complex interaction with the surrounding medium, and the time-dependent topology of multiple bubble growth and overlap. Other visualization techniques do not produce images that clearly demonstrate these phenomena. Our numerical simulations, coupled with the effective visualization techniques that we describe here, will allow us to make predictions for the *James Webb Space Telescope (JWST)*, planned for launch in $\sim$ 2013. The *JWST*, the key astronomy mission in the next decade, is extremely sensitive at near-infrared (NIR) wavelengths, where most of the light from the first stars, emitted at the source in the UV, but subsequently redshifted by the cosmic expansion into the NIR, is expected to reside.

The remainder of the paper is organized as follows: in Section 2 we present the cosmological motivation for our visualization; in Section 3 we describe our visualization process, and in Section 4 we discuss the insights made possible by our visualizations. We present related work in Section 5 and future work in Section 6.

2 Cosmological Background

2.1 Simulations

To study how the formation of the first stars affects the early universe, we carry out detailed three-dimensional simulations of a large volume of the cosmos during the epoch of the formation of the first generation of stars. These simulations allow us to follow the evolution of the primordial gas as it collapses under the influence of gravity to form stars, and as the radiation from these stars, in turn, alters the chemistry and thermal state of the gas.

2.1.1 Smoothed Particle Hydrodynamics

We carry out our simulations using the smoothed-particle hydrodynamics (SPH) code GADGET, in which the gas is modeled as discrete particles, each of which carries information about the dynamical, thermal, and chemical properties of the gas at a given point[17][16]. The mass contained in a given particle, however, is smoothed out over a volume that depends on the mass density and the numerical resolution. Variables at any given point in the fluid, and not only at the location of the particles, can then be estimated by kernel interpolation. Our simulation uses $\sim$ 2 million SPH particles, along with $\sim$ 2 million dark matter particles, which capture the gravitational effects that dark matter imposes. The volume of our cosmological simulation is a cubic box with side length[1] 460 kpc $(1+z)^{-1}$ h^{-1}, where z is the cosmological redshift, which decreases with time as the universe expands, and $h = 0.7$ is the Hubble constant in units of 100 km s^{-1} Mpc^{-1}, which describes the rate of the cosmic expansion.

We initialize our simulation at a redshift of $z = 99$, when the primordial gas is nearly uniformly distributed across space and each SPH particle modeling the gas has a density, temperature, and chemical abundances as derived from Big Bang theory and cosmological observations. As the gas in our cosmological volume evolves, we track the detailed evolution of the gas as it collapses, cools, and begins to form stars at a redshift $z \sim 20$, or $\sim$ 200 million years after the Big Bang.

2.1.2 Radiation From the First Stars

We model the effects of the radiation from the first generations of stars by placing point sources of radiation at the sites in our simulation where the gas collapses to high densities under the influence of gravity. The radiation from the first stars has two important effects on their surroundings, the ionization and concomitant heating of the primordial gas, and the destruction of the H_2 molecules in the gas, which are important coolants allowing the gas to collapse and form stars. The gas within a few kiloparsecs of the star is ionized and heated to temperatures above $\sim 10^4$ K, whereas the H_2 in the gas is destroyed within a slightly larger region around the star.

We use a ray-tracing method to find the exact structure of these two regions around the sites of star formation in our simulation. Within the so-called H II region, inside of which the gas is completely ionized, we set the electron fraction of the gas to unity and raise the temperature of the gas accordingly. Within the Lyman-Werner (LW) bubble, the region in which the molecules in the gas are destroyed, we set the fraction of H_2 to zero. Because the first stars are expected to have been very massive, with masses perhaps 100 times that of the Sun, we take it that the stars in our simulation have correspondingly short lifetimes of 3 Myr. Thus, after this brief stellar lifetime has elapsed in our simulation, we allow the gas to evolve once more without any radiative effects. In our simulation, eight stars are formed in the course of 50 Myr, and we carry out this detailed process of including the radiative effects for each of these stars.

2.2 Data Types

Each of the SPH particles that we use to model the primordial gas carries all of the relevant information that we would like to know about the dynamical, thermal, and chemical properties of the gas. In particular, each of these particles tracks the location, temperature, density, molecule (H_2) fraction, and electron fraction of a given parcel of gas. It is these properties of the primordial gas which are perhaps the most important to know in order to understand the process of the formation of the first stars and protogalaxies. Therefore, we have focused on visualizing these properties of the gas as they vary within our cosmological box, in order to extract an understanding of some of the many phenomena that arise with the feedback imposed by the first generations of stars.

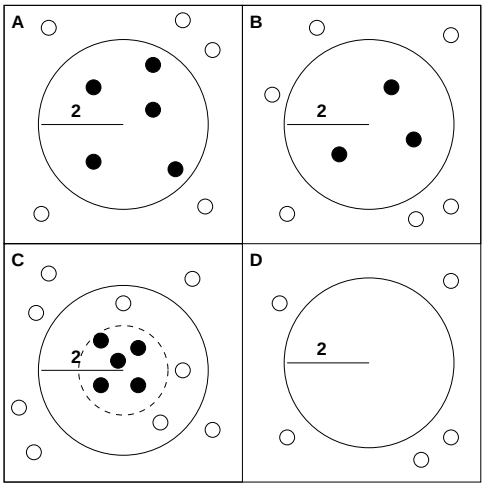

Figure 2: Our Local Interpolation Method — we show four cases to illustrate how our interpolation method works for distance $d = 2$ and $k = 5$, projected into two dimensions. In (**A**), exactly five particles are within the sampling radius d, and these five particles are used in the interpolation. In (**B**), only three particles are within the sampling radius, so only these three particles are used. In (**C**), there are eight particles within the sampling radius, so only the five ($k = 5$) closest are used. In (**D**), no particles are within the sampling radius, so default (in our case, zero) values are put at the interpolation point.

[1]The customary unit of distance in astronomy is the parsec, where 1 pc $= 3.09 \times 10^{16}$ m $= 3.26$ lightyears.

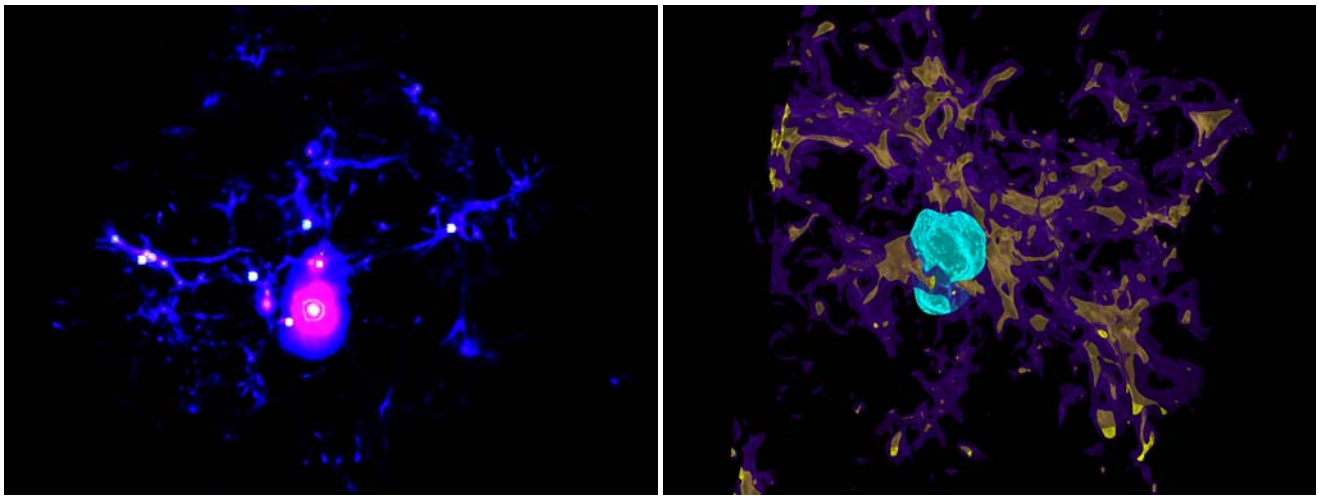

Figure 3: Technique Comparison — here we compare the image quality possible with our interpolation technique with an image taken directly from the simulation particle data. Both images show the density field in our simulation, while the right image also shows the electron fraction in an ionized region (cyan contour). The left image was generated directly from our particle data using alpha-blended sprites in Partiview[11]. The right image was generated by resampling our particle data to a regular grid using the interpolation we describe in Section 3. We then use ParaView[10] to extract and smooth the isosurfaces. In the right image, the full extent of the gas structures are visible, and the spatial relationships among the structures are clearly defined. Note that the transparency of the isosurfaces provides additional structural information without sacrificing the clarity of the spatial relationships.

3 Visualization Process

The most effective visualization of the data from our particle simulation will permit us to see the detailed structure of the gases and their spatial relationships. In particular, we would like to observe whether the ionized "bubbles" form in regions of high molecular density, and if hydrogen is suppressed in areas of active ionization. We would also benefit if the visualization revealed details of our simulation that we did not expect. The technique described below provides us with high-quality, detailed images that both confirm our original hypotheses and have led to new understanding. We describe the visualization technique here and the cosmological insight made possible by these visualizations in Section 4.

We initially visualized the particles directly using alpha-blended sprites at each particle location using Partiview[11], but the images generated did not clearly show the extent and detail of the gas structures. As can be seen on the left side of Figure 3, the resulting images from this technique lack sufficient depth to interpret the three dimensional relationships among the structures. Also, the structures themselves are not complete: because we are simulating gases, the particles with given variable value only partially define the extent of that structure in space. We want to extract the our desired isosurfaces from the particle data to find the full extent of the structures, and to make the spatial relationships among the structures more visible (as on the right side of Figure 3).

Most isosurface extraction techniques operate only on a grid, whether structured or unstructured[12]. Further, to obtain visualizations quickly, we want to use an existing visualization package rather than writing our own. Therefore, we resample our data onto a regular grid, which maximizes not only the applicable isosurface extraction techniques, but also the number of existing visualization packages that implement such techniques.

While many visualization packages implement isosurface extraction techniques, few contain any resampling methods. The Visualization ToolKit (VTK)[9] contains only two, the most appropriate of which is based on Shepard's method[15]. However, this interpolation is a global technique (performs n^2 interpolation) and is unacceptably slow for large data sets. For each interpolation sample, we want to include only the closest particles that most affect the value of the sample, while limiting the total number of particles considered for each sample so that we do not oversample in dense particle regions.

Jensen's photon mapping algorithm[6], a global illumination technique in computer graphics, uses an interpolation similar to what we want. In photon mapping, radiance samples are propagated from light sources to surfaces in a scene prior to any visibility calculations. The radiance at each sample is calculated using the lumination properties of the light source, the surface material properties, and the distance and angle between light and surface. These radiance samples are stored in a spatial acceleration structure. When rendering the scene, the indirect diffuse illumination on a surface is estimated by interpolating among the radiance samples near the visibility sample point. Jensen and Christensen[7] extend this technique to sample radiance in three dimensions, both on surfaces and in participating media. We adapt this three-dimensional interpolation technique to resample our particle data to a regular grid.

We perform the following steps in our process:

- **determine grid resolution** — the grid resolution is determined by a ratio of the density of points over the volume of the space that encloses them. To determine the number of cells per unit distance, we use the formula

$$\frac{3 \times n^{\frac{1}{3}}}{\Delta_{major\_axis}} \tag{1}$$

  where n is the number of particles in the original data set and Δ_{major_axis} is the length of the longest axis of the bounding box around the original data set. This value is multiplied by the length of each side of the bounding box to determine the final grid resolution along each axis. The grid resolution can also be specified by the user, which is useful to create a resampling at a lower level of detail than the original data set.

- **insert particles into grid** — once the grid resolution has been determined, the points are inserted into the grid according to their location in space. This grid both determines the sample

locations for the interpolation (at the vertices of each grid cell) and accelerates the identification of particles that should be included in each interpolation step. Our interpolation is bound by a distance d. If not set by the user, d is the length of the major axis of a cell.

- **interpolate data to grid vertices** — after the particles have been inserted into the grid, we perform an inverse-distance weighted interpolation at each vertex of the grid over the particles no further than d units away from the interpolation point. To prevent over-sampling in dense particle regions, we limit the interpolation to only the k particles closest to the interpolation point. If not set by the user, k is set equal to one percent of the total number of particles in the original data set. Figure 2 demonstrates the four possible scenarios where d and k may limit the number of particles used at an interpolation point. Note that if a global interpolation is desired, the user can set d equal to the major axis of the bounding box of the entire data set and set k equal to the total number of particles in the original data set.

For this paper, we use a $128 \times 128 \times 128$ grid with default d and k values ($d = 3.6$, $k = 20000$). The grid resolution is coarser than the default (384^3), which in our experience yields a smaller regular-grid data set without perceptible loss of visualization quality. The smaller grid is easier to load and manipulate, which results in faster generation of the visualizations.

After the interpolation is performed, we import the resulting regular grid into ParaView[10] to extract and smooth the isosurfaces. We choose ParaView because it is a mature, full-featured and open-source visualization package. Thus, our visualization method is widely usable because it does not rely on any proprietary software.

We use the default isosurface generation routine in ParaView (`vtkContourFilter`) to generate our isosurfaces. To ensure all isosurfaces are visible, we create only two to three isosurfaces per visualized variable. Low-value isosurfaces are colored darker and have greater transparency (lower alpha), whereas high-value isosurfaces are colored lighter and have greater opacity (higher alpha). For two-isosurface images, we use alpha values of 0.4 and 0.8; for three-isosurface images, we use alpha values of 0.3, 0.5, and 0.8. We select power-of-two increments for isosurface hue (e.g., 64, 128, 255), to visually distinguish isosurfaces of the same variable. In general, we use a standard color scheme to easily identify the variables in the visualization (green for hydrogen density, blue for molecular density, gray for ionized molecules; see Figures 4, 5, and 6); however, for dramatic effect in stand-alone images, we select high-contrast hues (see Figures 1 and 3).

After creating the isosurfaces, we apply a smoothing filter (`vtkSmoothPolyDataFilter`) to remove noise and insignificant surfaces from the isosurface extraction. We use 1000 iterations of the smoothing filter for the images in this paper. In Figure 5, we demonstrate the improvement in image quality that the smoothing filter provides. It is easier to see the significant structures in the smoothed image, and the spatial relationships among the structures are more readily apparent.

ParaView also incorporates animation controls, with which we create image sequences across our data sets. By creating a time series in ParaView, we create the desired isosurfaces for one time step and generate tens to hundreds of images across the sequence.

4 Results and Discussion

The visualizations produced by our technique provide us with critical insight into the structure and spatial organization of the gases in our simulation, which furthers our cosmological understanding and the impact of our work. We describe several of these cosmological insights below.

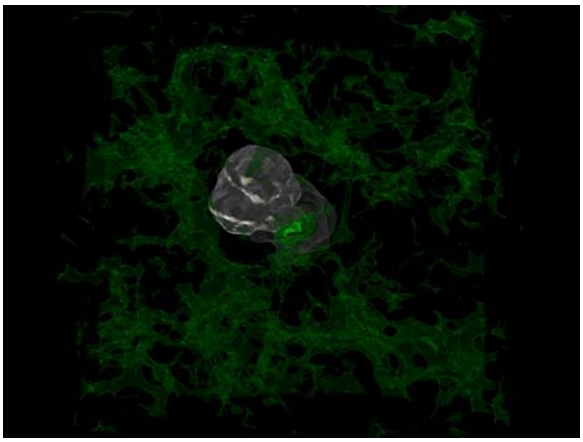

Figure 4: Hydrogen Ionization — This figure shows an active and a "ghost" ionized region,wherein recombination is taking place and the gas is again becoming neutral, along with the molecular hydrogen (H_2) fraction within our simulation. Ionized gas isosurfaces $5e^{-2}$ (opaque) and $5e^{-3}$(transparent) are in gray, and hydrogen density isosurfaces $3e^{-6}$, $1e^{-5}$, and $1e^{-4}$ are in green Notice that the H_2 fraction is suppressed around the active ionized region, but is instead elevated within the "ghost" ionized region.

4.1 Cosmological Insights

The key question for cosmology is to understand the fundamental transition in the early universe from simplicity to complexity, brought about by the first stars. Specifically, how was the universe re-ionized, and how was it enriched with the first heavy elements? Understanding the build-up of ionized regions around the first stars is important for a number of reasons. Firstly, the evolution of the ionized bubbles, the speed with which they grow, and the final size reached, are diagnostic of the properties of the first stars, in particular their mass. The typical mass of the first stars is currently only predicted by theory, and it is essential to devise empirical tests. One such test is to carry out simulations of the early re-ionization process, assuming different stellar masses, and to trace and characterize the resulting pattern of ionized bubbles. The observational signature includes the three-dimensional arrangement of the bubbles, their clustering properties, and their overall volume filling fraction as a function of time. Visualizations are crucial to glean this signature from the numerical simulations. Our visualizations have shown that the bubble interior is not uniformly ionized (see Figure 1); instead there are pockets of high-density gas inside of them that remain substantially neutral. We find that higher mass stars tend to result in more homogeneous bubble interiors. In addition, higher mass stars produce larger ionized bubbles that fill a larger fraction of the available cosmic volume. Note that the structural detail found in our isosurface visualizations enables these observations, observations that are not possible with direct visualization on the particles.

Secondly, the build-up of bubbles is related to what is termed "radiative feedback". The basic idea is that stars can only form out of cold, dense gas. Once the first stars have formed, they ionize and heat the surrounding medium, so that no other, secondary stars can form for a substantial amount of time. Put differently: wherever the ionized bubbles extend, further star formation is suppressed. Visualizing the network of radiation bubbles is therefore crucial to characterize the strength of this negative feedback. More precisely, there are two different kinds of radiation bubbles surrounding the first stars: hard UV photons that are capable of ionizing hydrogen atoms, and somewhat less energetic, soft UV photons that are capable of dissociating hydrogen molecules. The latter are very

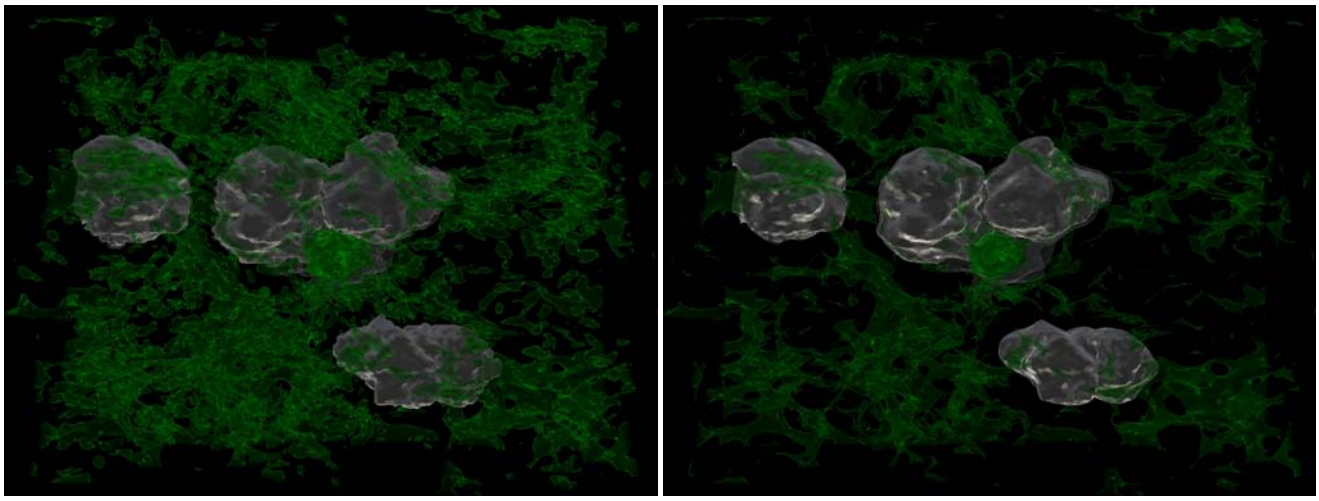

Figure 5: Isosurface Extraction and Smoothing — These figures show several active and one "ghost" ionized region, wherein recombination is taking place and the gas is again becoming neutral, along with the molecular hydrogen (H_2) fraction within our simulation. The left image contains raw isosurfaces, and the right image contains isosurfaces after the application of a smoothing filter. The smoothing filter sharpens the significant structures and removes the insignificant structures, making the spatial relationships among the structures more readily apparent.

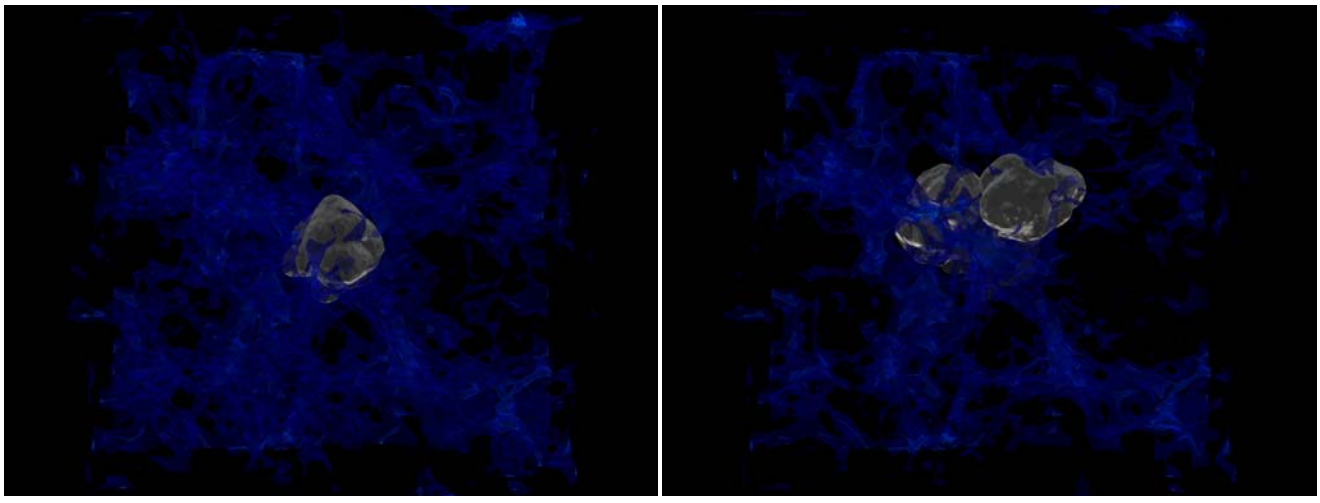

Figure 6: Formation of Ionized Regions — This figure shows the density field when the first star has formed (left) and after a second and third star have formed (right). Notice that in the right image, the first star has turned off and only the "ghost" ionized region is present (parially obscured by the molecular density isosurfaces). Ionized gas isosurfaces $5e^{-2}$ (opaque) and $5e^{-3}$(transparent) are in gray, and density isosurfaces $1.1e^{-2}$ and $5e^{-3}$ are in blue. Notice that the second and third stars have formed in the densest regions, as expected.

important, because they cool the primordial gas, thus enabling the formation of the first stars. The extent of the soft-UV bubbles thus delineates regions where no stars can form. We find the surprising result that soft UV photons seem much less effective in shutting off secondary star formation than was previously thought. Our visualizations clearly show the relation of the two classes of UV bubbles: The soft UV bubbles are larger than the hard UV ones, but, surprisingly, only slightly so, as can be seen in Figure 4. As this figure demonstrates, the smoothing filter and transparency used in our visualization is essential for drawing new cosmological insights.

A related question concerns the overall time evolution of early re-ionization. Traditionally, it has been argued that re-ionization is a strictly monotonous process. The fraction of the volume filled by ionized bubbles was thought to only increase with time. Our work has shown that the early stages of re-ionization occur in a much more complex fashion, where bubbles grow, disappear again, and are eventually replaced by new bubbles. The time evolution, therefore, is highly intermittent, and not at all monotonic. This effect can be seen in Figure 6, where the ionized region of the first star has been largely replaced by the ionized regions of the second and third star. Note that these observations cannot be made without seeing the spatial relationships that are made clear in our visualizations.

Our visualizations also have allowed us to understand this intermittency more fully. Specifically, we find that the bubbles do not disappear completely after the star that produced them has died; instead, a remnant of reduced, but still significant, ionization lingers on for a long time (see Figure 1), so that a given point in space can be influenced simultaneously by such a "ghost" bubble, together with a freshly formed bubble around a star that is still alive, as can be seen in Figures 4 and 6. Again, the observational signature form the early re-ionization, which depends on the precise degree of ionization, looks substantially different because of this "ghost" effect. Transparency and smoothing are necessary to observe these structural details.

An effect related to the intermittecy of the ionization at the early stages of star formation is the production of a high molecular hydrogen (H_2) fraction within the "ghost" ionized regions. This occurs because the small degree of ionization that lingers in these regions allows for free electrons to catalyze the production of H_2. The high fraction of H_2 that develops in one of these regions can be seen in Figure 4, where the highest H_2 fraction is clearly shown within the "ghost" ionized region in the middle of our simulation box. Because molecules are effective coolants of the gas, these regions may be the sites of continued star formation, a further illustration of how the UV radiation from the first stars is surprisingly ineffectual at suppressing star formation.

5 Related Work

While a lengthy discussion of interpolation techniques and isosurface extraction methods is beyond the scope of this paper, we provide an overview below.

5.1 Isosurface Extraction

Most isosurface extraction methods operate only on structured data (usually a structured grid). The most well-known of these techniques is Marching Cubes[14] and the octree-based improvement to it[19]. Value-space decomposition techniques, such as NOISE[13] and interval trees[3][2], can extract isosurfaces from datasets that lack structure. Methods based on particle attraction also exist[4]. Livnat provides a good overview of popular techniques[12], and Sutton, et. al., have evaluated the performance of a number of isosurface extraction techniques[18].

5.2 Interpolation Techniques

Franke[5] provides an overview and evaluation of a number of interpolation techniques. He categorizes interpolation methods according to the interpolant used, include inverse distance weighted methods, rectangle-based blending methods, triangle-based blending methods, finite-element-based methods, Foley's methods, and Nodal basis function methods. Further, these techniques can be broken into *global* techniques that perform n^2 interpolation, and *local* techniques that limit the number of points in the interpolation to a local region around each sample point. Our technique would be categorized as a local inverse distance weighted method, which is a generalization of Shepard's method[15].

6 Conclusion and Future Work

In this paper, we describe our method of visualizing cosmological point-based datasets. This method is simple, flexible, and leverages existing visualization software. We demonstrate that our isosurface-based visualization provides detail and clarity superior to that of a direct visualization of the particle data.

With this visualization we have gained a clearer view of the effects of the radiation from the first stars, allowing a detailed description of the early development of the ionized regions that are created around these first sources of light, as well as illustrating how star formation can continue despite the suppressive effects of the radiation. The details of early star formation that we are able to glean using our method of visualization will allow us to make improved predictions for what the *James Webb Space Telescope*, the key astronomy mission of the next decade, will discover in the early universe, probing the formative first billion years of cosmic history.

Further, we are applying our technique to the visualization of other early universe phenomena. We have begun to visualize a simulation of the first supernova explosion, and our technique has produced similar improvement in our image quality and the insights possible because of them.

Acknowledgements

Thanks to Karla Vega at TACC for providing the alpha-blended particle image in Figure 3. Our cosmological particle simulation was funded in part by NASA *Swift* grant NNG05GH54G.

References

[1] V. Bromm and R. Larson. The first stars. *Annual Review of Astronomy & Astrophysics*, 42:79–118, 2004.

[2] P. Cignoni, P. Marino, C. Montani, E. Puppo, and R. Scopigno. Speeding up isosurface extraction using interval trees. *IEEE Transactions on Visualization and Computer Graphics (TVCG)*.

[3] P. Cignoni, C. Montani, E. Puppo, and R. Scopigno. Optimal isosurface extraction form irregular volume data. In *Volume Visualization 1996 (Proceedings of the 1996 Symposium on Volume Visualization)*, pages 31–38, 1996.

[4] P. Crossno and E. Angel. Isosurface extraction using particle systems. In *Visualization '97 (Proceedings of IEEE Vis 1997)*, pages 495–498, 1997.

[5] R. Franke. Scattered data interpolation: Tests of some methods. *Mathematics of Computation*, 38(157):181–200, January 1982.

[6] H. W. Jensen. Global Illumination using Photon Maps. in X. Pueyo and P. Schröder, editors, Rendering Techniques '96, pages 21–30. Springer-Verlag, 1996.

[7] H. W. Jensen and P. H. Christensen. Efficient simulation of light transport in scenes with participating media using photon maps. In *Proceedings of the 25th annual conference on Computer graphics and interactive techniques (ACM SIGCGIT)*, pages 311–320, 1998.

[8] J. L. Johnson, T. H. Greif, and V. Bromm. Local radiative feedback in the formation of the first protogalaxies. *The Astrophysical Journal*, 2007 *submitted*.

[9] Kitware Incorporated. The Visualization ToolKit (VTK) 5.0 (*http://www.vtk.org/*), 2007.

[10] Kitware Incorporated, Los Alamos National Laboratory, and Sandia Corporation. ParaView 2.6.0 (*http://www.paraview.org/*), 2007.

[11] S. Levy. Partiview 0.89 (*http://dart.ncsa.uiuc.edu/partiview/*), 2006.

[12] Y. Livnat. Accelerated Isosurface Extraction Approaches. in C. Hansen and C. Johnson, editors, The Visualization Handbook, pages 39–55. Elsevier, 2005.

[13] Y. Livnat, H.-W. Shen, and C. R. Johnson. A near optimal isosurface extraction algorithm using the span space. *IEEE Transactions on Visualization and Computer Graphics (TVCG)*, 2(1):73–84, March 1996.

[14] W. E. Lorensen and H. E. Cline. Marching cubes: A high resolution 3d surface construction algorithm. In *Computer Graphics (Proceedings of SIGGRAPH 87)*, volume 21, pages 163–169, July 1987.

[15] D. Shepard. A two-dimensional interpolation function for irregularly-spaced data. In *Proceedings of the 1968 23rd ACM national conference*, pages 517–524, 1968.

[16] V. Springel and L. Hernquist. Cosmological smooth particle hydrodynamics simulations: the entropy equation. *Monthly Notices of the Royal Astronomical Society*, 333:649, 2002.

[17] V. Springel, N. Yoshida, and S. White. Gadget: a code for collisionless and gasdynamical cosmological simulations. *New Astronomy*, 6:79, 2001.

[18] P. Sutton, C. Hansen, H. Shen, and D. Schikore. P. sutton, c. hansen, h.-w. shen, and d. schikore. a case study of isosurface extraction algorithm performance. in w. de leeuw and r. van liere, editors, data visualization 2000, pages 259–268. springer, 2000., 2000.

[19] J. Wilhelms and A. V. Gelder. Octrees for faster isosurface generation. In *ACM Transactions on Graphics (TOG)*, volume 11, pages 201–227, 1992.